

HRh(dppb)₂, a Powerful Hydride Donor

Andrew J. Price,[†] Rebecca Ciancanelli,[†] Bruce C. Noll,[†] Calvin J. Curtis,[‡]
Daniel L. DuBois,^{*,‡} and M. Rakowski DuBois^{*,†}

Department of Chemistry and Biochemistry, University of Colorado, Boulder, Colorado 80309,
and the National Renewable Energy Laboratory, 1617 Cole Boulevard,
Golden, Colorado 80401

Received May 28, 2002

The Rh(I) and Rh(III) hydrides HRh(dppb)₂ and [HRh(dppb)₂(NCCH₃)](BF₄)₂ (where dppb is 1,2-bis(diphenylphosphino)benzene) have been prepared, and a structural study of [HRh(dppb)₂(NCCH₃)](BF₄)₂ has been completed. The latter complex is an octahedral complex with a trans arrangement of the hydride and acetonitrile ligands. A pK_a value of 9.4 was measured for this complex by equilibration of [Rh(dppb)₂](BF₄) with 4-bromoanilinium tetrafluoroborate in acetonitrile. [Rh(dppb)₂](BF₄) reacts with H₂ in the presence of Pt(dmpp)₂, which acts as a base, to form HRh(dppb)₂ and [HPt(dmpp)₂](BF₄) (where dmpp = 1,2-bis(dimethylphosphino)propane). An equilibrium constant of 0.42 ± 0.2 was measured for this reaction. Using this equilibrium measurement and a thermodynamic cycle, the hydride donor ability (ΔG_{H⁻}) of HRh(dppb)₂ was determined to be 34 kcal/mol. This value indicates that HRh(diphosphine)₂ complexes are powerful hydride donors. Similarly the pK_a value of HRh(dppb)₂ was calculated to be 35 from a thermodynamic cycle that included the potential of the Rh(I/–I) couple (E_{1/2} = –2.02 V vs ferrocene). These results combined with results from the literature suggest the following order of hydricity for five-coordinate, 18-electron hydrides: second row > third row > first row. Similarly an acidity order of second row ≥ first row > third row is deduced.

Introduction

Rhodium hydride complexes are intermediates in a variety of catalytic reactions.¹ In general, rhodium complexes appear to be more reactive than their cobalt and iridium analogues, but the origin of this enhanced reactivity is not fully understood. Although these differences in reactivity may be related to thermodynamic differences of the M–H bond, limited data are available. Acidity data² and homolytic bond dissociation energies³ for rhodium hydride complexes are scarce, and no data are available on the relative ability of rhodium hydride derivatives to act as hydride donors.

Previous studies of [HNi(diphosphine)₂]⁺ and [HPt(diphosphine)₂]⁺ complexes indicate that the platinum complexes are more hydridic than their nickel ana-

logues, but no data could be obtained for the analogous palladium hydrides, which are unstable with respect to H₂ elimination.⁴ For CpMo(CO)₃H and CpW(CO)₃H the hydricity appears to be greater for W than for Mo,⁵ but the hydricities of Cp₂NbH₃ and Cp₂TaH₃ have been reported to be the same.⁶ This leaves the situation of the relative hydricities of first, second, and third row transition metals unclear, but suggests that the ordering may be different for different geometries and ligands. In this paper we report the measurement of the acidity and hydricity of HRh(dppb)₂ and compare these values with those determined previously for [HM(diphosphine)₂]ⁿ complexes of cobalt (n = 0) and platinum and nickel (n = 1+). HRh(dppb)₂ has the greatest hydride donor ability of any of the complexes that we have studied to date.

Results

Synthesis and Characterization of Complexes.

The complexes [Rh(dppb)₂][BF₄] and [Rh(dppe)₂][BF₄] have been previously prepared.^{7,8} The dppb derivative proved to be most suitable for our studies, for reasons discussed below, and characterization data that were not reported previously are presented here. The ³¹P

[†] University of Colorado.

[‡] National Renewable Energy Laboratory.

(1) (a) Osborn, J. A.; Jardine, F. H.; Young, J. F.; Wilkinson, G. *J. Chem. Soc. A* **1966**, 1711. (b) Vineyard, B. D.; Knowles, W. S.; Sabacky, M. J.; Bachman, G. L.; Weinkauff, D. *J. Am. Chem. Soc.* **1977**, *99*, 5946. (c) Kagan, H. B.; Dang, T.-P. *J. Am. Chem. Soc.* **1972**, *94*, 6429. (d) Evans, D.; Yagupsky, G.; Wilkinson, G. *J. Chem. Soc. A* **1968**, 2660. (e) Fowler, R.; Connor, H.; Baehl, R. A. *Chem. Technol.* **1976**, 772.

(2) (a) Kristjánssdóttir, S. S.; Norton, J. R. In *Transition Metal Hydrides*; Dedieu, A., Ed.; VCH: New York, 1991; pp 309–359. (b) Schrauzer, G. N.; Holland, R. J. *J. Am. Chem. Soc.* **1971**, *93*, 1505. (c) Pearson, R. G.; Kresge, C. T. *Inorg. Chem.* **1981**, *20*, 1878. (d) Halpern, J.; Riley, D. P.; Chan, A. S. C.; Pluth, J. J. *J. Am. Chem. Soc.* **1977**, *99*, 8055. (e) Ramasami, T.; Espenson, J. H. *Inorg. Chem.* **1980**, *19*, 1846. (f) Gillard, R. D.; Heaton, B. T.; Vaughan, D. H. *J. Chem. Soc., A* **1970**, 3126.

(3) (a) Wayland, B. B.; Coffin, V. L.; Farnos, M. D. *Inorg. Chem.* **1988**, *27*, 2745. (b) Coffin, V. L.; Brennen, W.; Wayland, B. B. *J. Am. Chem. Soc.* **1988**, *110*, 6063. (c) Wei, M.; Wayland, B. B. *Organometallics* **1996**, *15*, 4681–4683. (d) Simões, J. A. M.; Beauchamp, J. L. *Chem. Rev.* **1990**, *90*, 629–688.

(4) (a) Berning, D. E.; Noll, B. C.; DuBois, D. L. *J. Am. Chem. Soc.* **1999**, *121*, 11432–11447. (b) Berning, D. E.; Miedaner, A.; Curtis, C. J.; Noll, B. C.; Rakowski DuBois, M.; DuBois, D. L. *Organometallics* **2001**, *20*, 1832–1839.

(5) Sarker, N.; Bruno, J. W. *J. Am. Chem. Soc.* **1999**, *121*, 2174–2180.

(6) Sarker, N.; Bruno, J. W. *Organometallics* **2001**, *20*, 55–61

(7) Fordyce, W. A.; Crosby, G. A. *Inorg. Chem.* **1982**, *21* (4), 1455.

(8) van der Ploeg, A. F. M. J.; Van Koten, G. *Inorg. Chim. Acta* **1981**, *51*, 225–239.

Table 1. Selected Bond Distances (Å) and Angles (deg) for $[\text{HRh}(\text{dppb})_2(\text{CH}_3\text{CN})][\text{BF}_4]_2 \cdot 2\text{CH}_3\text{CN}$

Bond Distances			
Rh(1)–H(1)	1.51(5)	Rh(1)–N(1)	2.119 (4)
Rh(1)–P(1)	2.3493(10)	Rh(1)–P(2)	2.3493 (11)
Rh(1)–P(3)	2.3621(11)	Rh(1)–P(4)	2.3613 (11)
N(1)–C(61)	1.130(6)	C(1)–C(2)	2.215 (6)
P(1)–C(3)	2.393(7)	P(2)–C(4)	2.462 (7)

Bond Angles			
N(1)–Rh(1)–P(1)	77.64 (6)	N(1)–Rh(1)–P(2)	86.17 (6)
N(1)–Rh(1)–P(3)	76.70 (16)	N(1)–Rh(1)–P(4)	80.88 (6)
H(1)–Rh(1)–P(1)	118.9 (2)	H(1)–Rh(1)–P(2)	79.8 (18)
H(1)–Rh(1)–P(3)	88.9 (17)	H(1)–Rh(1)–P(4)	92.4 (17)
H(1)–Rh(1)–N(1)	177.0 (17)	P(1)–Rh(1)–P(4)	97.33 (4)
P(1)–Rh(1)–P(2)	81.68 (4)	P(3)–Rh(1)–P(4)	83.71 (4)
P(2)–Rh(1)–P(3)	96.80 (4)		

NMR spectrum of $[\text{Rh}(\text{dppb})_2][\text{BF}_4]$ exhibits a doublet centered at 62.5 ppm ($^1J_{\text{P-Rh}} = 134$ Hz). This chemical shift and coupling constant are consistent with a chelating phosphine bound to Rh(I).⁹ The electrospray mass spectrum ($m/z = 995$) is also consistent with a $[\text{Rh}(\text{dppb})_2]^+$ cation.

Reaction of $[\text{Rh}(\text{dppb})_2][\text{BF}_4]$ with LiAlH_4 in toluene gives the neutral rhodium hydride complex $\text{HRh}(\text{dppb})_2$ in fair yield. The ^{31}P NMR spectrum consists of a doublet of doublets centered at 59.3 ppm ($^1J_{\text{P-Rh}} = 142$ Hz, $^2J_{\text{P-H}} = 18$ Hz). The hydride region of the ^1H NMR spectrum shows a doublet of pentets at -9.4 ppm as expected for a fluxional five-coordinate species ($^1J_{\text{Rh-H}} = 12$ Hz, $^2J_{\text{P-H}} = 18$ Hz). The infrared absorption spectrum has a band at 1868 cm^{-1} assigned to the Rh–H stretch. The deuterated analogue, $\text{DRh}(\text{dppb})_2$, was prepared by reacting LiEt_3BD with $[\text{Rh}(\text{dppb})_2][\text{BF}_4]$. A new infrared absorption band is observed at 1343 cm^{-1} for the deuterium-labeled complex, and that at 1868 cm^{-1} is absent, consistent with the expected shift in the infrared spectrum.

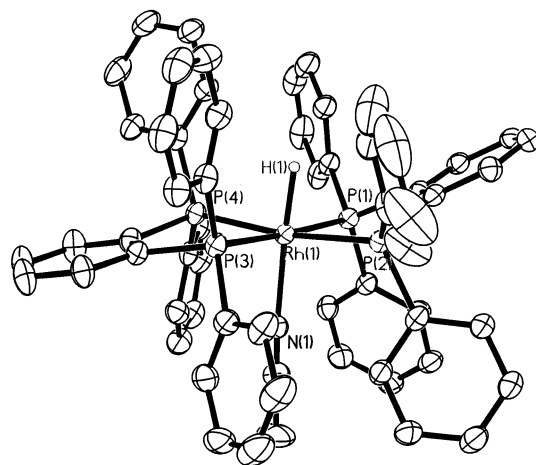
Reaction of $[\text{Rh}(\text{dppb})_2][\text{BF}_4]$ in acetonitrile with a stoichiometric amount of ethereal tetrafluoroboric acid gave a new compound formulated as $[\text{HRh}(\text{dppb})_2(\text{CH}_3\text{CN})][\text{BF}_4]_2$. This compound is a colorless solid, with a doublet in the ^{31}P NMR spectrum at 56.8 ppm ($^1J_{\text{P-Rh}} = 93$ Hz). The phosphorus spectrum is consistent with an octahedral structure in which the hydride and acetonitrile ligands are trans and all four phosphorus atoms are equivalent. Supporting this structural assignment is the observation that the hydride resonance in the ^1H NMR spectrum is a doublet of pentets (-14.6 ppm, $^1J_{\text{Rh-H}} = 10$ Hz, $^2J_{\text{P-H}} = 7.5$ Hz). A broad and weak infrared band at 1993 cm^{-1} is tentatively assigned to the Rh–H stretch.

Crystallization of $[\text{HRh}(\text{dppb})_2(\text{CH}_3\text{CN})][\text{BF}_4]_2$ from a mixture of acetonitrile and diethyl ether gave crystals that were suitable for X-ray diffraction studies. Selected bond distances and angles and crystallographic data are shown Tables 1 and 2, respectively. The molecular structure of $[\text{HRh}(\text{dppb})_2(\text{CH}_3\text{CN})][\text{BF}_4]_2$ confirms the assigned octahedral structure as shown in Figure 1. The four phosphorus atoms bend toward the hydride ligand as indicated by an average N–Rh–P bond angle of $92.83(10)^\circ$. This distortion is expected for both electronic and steric reasons¹⁰ and is similar to that observed for $[\text{HCo}(\text{dppe})_2(\text{CH}_3\text{CN})][\text{BF}_4]_2$.¹¹ The Rh–N bond length

Table 2. Crystal Data for $[\text{HRh}(\text{dppb})_2(\text{CH}_3\text{CN})][\text{BF}_4]_2 \cdot 2\text{CH}_3\text{CN}$

formula	$\text{C}_{132}\text{H}_{116}\text{B}_4\text{F}_{16}\text{N}_6\text{P}_8\text{Rh}_2$
fw (amu)	2587.13
cryst syst	triclinic
unit cell dimens	
<i>a</i> (Å)	13.8411(18)
<i>b</i> (Å)	20.305(3)
<i>c</i> (Å)	22.832(3)
α (deg)	103.609(3)
β (deg)	98.905(3)
γ (deg)	96.007(3)
volume, Å ³	6094.5(14)
space group	<i>P</i> 1
<i>Z</i>	2
density, calc (mg/m ³)	1.410
λ (Mo K α) (Å)	0.71073
temp (K)	130 (2)
scan type	ϕ and ω scans
θ range	$0.93 < \theta < 26.37$
no. of ind reflns	24 831 ($R(\text{int}) = 0.0535$)
no. of reflns obsd	18 215
abs coeff, mm ⁻¹	semiempirical from equivalents
R^a	0.0814
R_w^b	0.1557
GOF ^c	1.031
largest peak in final diff map (e ⁻ /Å ³)	1.562 and -1.018

^a $R = R_1 = \sum |F_o| - |F_c| / \sum |F_o|$. ^b $R_w = [\sum [w(F_o^2 - F_c^2)^2] / \sum [w(F_o^2)^2]]^{1/2}$. ^c $\text{GOF} = S = [\sum [w(F_o^2 - F_c^2)^2] / (M - N)]^{1/2}$ where *M* is the number of reflections and *N* is the number of parameters refined.

**Figure 1.** Perspective drawing and numbering scheme for the cation of $[\text{HRh}(\text{dppb})_2(\text{CH}_3\text{CN})][\text{BF}_4]_2 \cdot 2\text{CH}_3\text{CN}$. Thermal ellipsoids are shown at 50% probability.

of 2.119(4) Å is normal for a second row metal complex of acetonitrile.¹² The Rh–P bond lengths ($\text{Rh-P}_{\text{av}} = 2.3555(11)$ Å) are slightly shorter than other reported trans Rh(III)–P bonds¹³ (e.g., $\text{Rh-P}_{\text{av}} = 2.398(4)$ Å in $\text{Rh}(\text{PPh}_3)_3\text{Cl}_3$).^{13a} The hydride ligand was located by a difference Fourier map, and a Rh–H bond distance of 1.51(5) Å was determined.

Electrochemical Studies of $[\text{Rh}(\text{diphosphine})_2][\text{BF}_4]$. A reversible two-electron reduction is observed

(10) (a) Elian, M.; Hoffmann, R. *Inorg. Chem.* **1975**, *14*, 1058–1076. (b) Wander, S. A.; Miedaner, A.; Noll, B. C.; Barkley, R. M.; DuBois, D. L. *Organometallics* **1996**, *15*, 3360–3373.

(11) Ciancanelli, R.; Noll, B. C.; DuBois, D. L.; Rakowski DuBois, M. *J. Am. Chem. Soc.* **2002**, *124*, 2984–2992.

(12) Storhoff, B. N.; Lewis, H. C., Jr. *Coord. Chem. Rev.* **1977**, *23*, 1–29.

(13) (a) Skapski, A. C.; Stephens, F. A. *J. Chem. Soc., Dalton Trans.* **1973**, 1789. (b) Allen, F. H.; Chang, G.; Cheung, K. K.; Lai, T. F.; Lei, L. M.; Pidcock, A. *Chem. Commun.* **1970**, 1297.

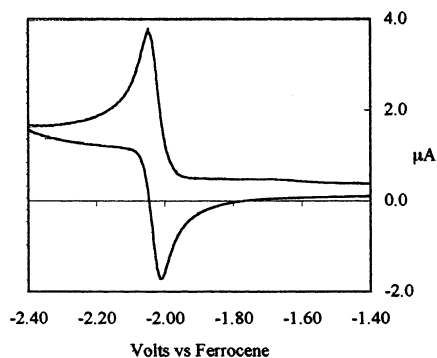
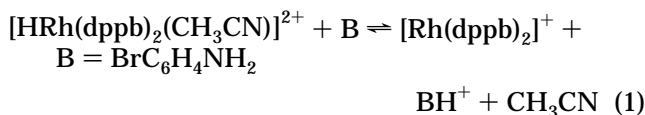


Figure 2. Cyclic voltammogram of $[\text{Rh}(\text{dppb})_2]^+$ in acetonitrile/0.3 M $n\text{-Bu}_4\text{NPF}_6$ at a scan rate of 50 mV/s.

at -2.02 V vs ferrocene for $[\text{Rh}(\text{dppb})_2]^+$ in acetonitrile as shown by the cyclic voltammogram in Figure 2. The observed reduction wave is diffusion-controlled, as indicated by a linear plot of the peak current vs the square root of the scan rate, and the observed peak-to-peak separation of 33 mV at 50 mV/s is near the 30 mV value expected for a two-electron reduction.¹⁴ The ratio of the cathodic to anodic peak currents of 0.95 at 50 mV/s is consistent with a fully reversible process. The geometry of the square-planar Rh(I) complex is expected to change to a distorted tetrahedron upon reduction based on the structures of other four-coordinate d^8 and d^{10} complexes.^{4,15} These rearrangements are rapid on the CV time scale at scan rates of 50–4000 mV/s. Similar electrochemical behavior is observed for $[\text{Rh}(\text{dppe})_2][\text{BF}_4]$, which was studied for comparison. A reversible two-electron reduction is observed at -2.12 V vs Fc. Reversible waves were not observed in the cyclic voltammograms of $\text{HRh}(\text{dppb})_2$ or $[\text{HRh}(\text{dppb})_2(\text{CH}_3\text{CN})]^{2+}$.

Thermodynamic Studies of the Rh–H Bond. Acidity of $[\text{HRh}(\text{diphosphine})_2(\text{CH}_3\text{CN})][\text{BF}_4]_2$ Derivatives. As discussed above, $[\text{Rh}(\text{dppb})_2][\text{BF}_4]$ reacts quantitatively with a stoichiometric amount of tetrafluoroboric acid to produce $[\text{HRh}(\text{dppb})_2(\text{CH}_3\text{CN})][\text{BF}_4]_2$. However, an equilibrium is observed when 4-bromoanilinium tetrafluoroborate is used as the acid. To confirm that the system is at equilibrium, the reaction was also run in the reverse direction, i.e., starting from $[\text{HRh}(\text{dppb})_2(\text{CH}_3\text{CN})][\text{BF}_4]_2$ and 4-bromoaniline, as shown in reaction 1. This reaction can be conveniently followed by ^{31}P NMR spectroscopy. Integration of the resonances of the two rhodium complexes provides a convenient method for determining the ratio of $[\text{HRh}(\text{dppb})_2(\text{CH}_3\text{CN})][\text{BF}_4]_2$ to $[\text{Rh}(\text{dppb})_2][\text{BF}_4]$. Integrations reached constant values over a period of 8 h. The conjugate pair of 4-bromoanilinium tetrafluoroborate and 4-bromoaniline were used in a 20-fold excess in a 1:1 ratio. Under these conditions, the protonation of $[\text{Rh}(\text{dppb})_2][\text{BF}_4]$ makes a negligible contribution to the ratio of protonated and unprotonated 4-bromoaniline. The results of four experiments, two in each direction, gave an equilibrium constant of 1.5 ± 0.3 for reaction 1.

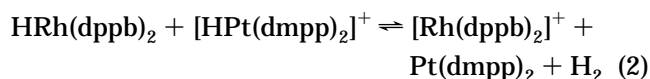


(14) Bard, A. J.; Faulkner, L. R. *Electrochemical Methods*; John Wiley & Sons: New York, 1980; pp 218 and 229.

In the calculation of this equilibrium constant, the participation of the solvent, acetonitrile, was neglected, i.e., the $K_{\text{eq}1} = [\text{BH}^+][\text{Rh}]/[\text{HRh}]$ (where $\text{Rh} = [\text{Rh}(\text{dppb})_2]^+$ and $\text{HRh} = [\text{HRh}(\text{dppb})_2(\text{CH}_3\text{CN})]^{2+}$). The $\text{p}K_{\text{a}}$ value of $[\text{HRh}(\text{dppb})_2(\text{CH}_3\text{CN})][\text{BF}_4]_2$ in acetonitrile (9.4 ± 0.3) was calculated by subtracting the log of this equilibrium constant from the $\text{p}K_{\text{a}}$ value of 4-bromoanilinium (9.6).¹⁶ This approach results in a $\text{p}K_{\text{a}}$ value that accurately reflects that $[\text{HRh}(\text{dppb})_2(\text{CH}_3\text{CN})]^{2+}$ will dissociate a proton in acetonitrile solution only slightly more than protonated 4-bromoaniline. It also allows the accurate prediction of the free energy for the reaction of this complex with other bases whose $\text{p}K_{\text{a}}(\text{BH}^+)$ values are known in acetonitrile.

A similar equilibrium measurement was carried out for the reaction of $[\text{HRh}(\text{dppe})_2(\text{CH}_3\text{CN})][\text{BF}_4]_2$ with 4-bromoaniline in acetonitrile, and the equilibrium constant was determined to be 4.1 ± 0.6 . This corresponds to a $\text{p}K_{\text{a}}$ value of 9.0 ± 0.3 .

Hydricity of $\text{HRh}(\text{dppb})_2$. The hydride donor ability of $\text{HRh}(\text{dppb})_2$ was obtained from equilibrium studies in benzonitrile of the reaction of $[\text{Rh}(\text{dppb})_2][\text{BF}_4]$ with H_2 in the presence of $\text{Pt}(\text{dmpp})_2$ to form $\text{HRh}(\text{dppb})_2$ and $[\text{HPt}(\text{dmpp})_2][\text{BF}_4]$ ($\text{p}K_{\text{a}} = 30.4$), the reverse of reaction 2.¹⁷



The relative ratios of the four metal complexes were determined by integration of the appropriate ^{31}P NMR resonances. The activity of hydrogen at 1.0 atm was taken as 1. An equilibrium constant of 2.4 ± 1.0 was measured for reaction 2 from a series of four experiments carried out in the reverse direction as described in the Experimental Section. The reversibility of reaction 2 was established by purging the solution with N_2 after equilibrium had been reached under hydrogen. In this case $\text{HRh}(\text{dppb})_2$ disappeared with reformation of $[\text{Rh}(\text{dppb})_2]^+$.

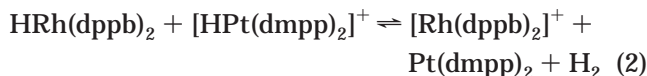
Although this equilibrium study was performed in benzonitrile for solubility reasons, we believe that it provides a good estimate of the equilibrium value in acetonitrile as well. A similar heterolytic cleavage reaction of $[\text{Pt}(\text{dmpp})_2][\text{BF}_4]_2$ with hydrogen and triethylamine was performed in both benzonitrile and acetonitrile and gave equilibrium constants of 3.2 ± 0.5 and 1.7 ± 0.3 , respectively, with corresponding values of $\Delta G_{\text{H}^-}^0$ of 51.4 and 51.0 kcal/mol, respectively. This indicates that the use of benzonitrile in place of acetonitrile should not introduce a large error in $\Delta G_{\text{H}^-}^0$. We estimate the difference in this value in the two solvents to be less than 0.8 kcal/mol on the basis of this result and previous results that compared equilibria involving proton transfer reactions in both solvents.⁴

(15) Longato, B.; Riello, L.; Bandoli, G.; Pilloni, G. *Inorg. Chem.* **1999**, *37*, 2818.

(16) Kristjánssdóttir, S. S.; Moody, A. E.; Weberg, R. T.; Norton, J. R. *Organometallics* **1988**, *7*, 1983–1987.

(17) Curtis, C. J.; Miedaner, A.; Ellis, W. W.; DuBois, D. L. *J. Am. Chem. Soc.* **2002**, *124*, 1918–1925.

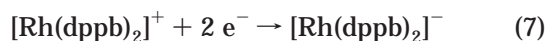
Reaction 2 can be combined with reactions 3 and 4 to produce a thermodynamic cycle whose sum is the heterolytic cleavage of the Rh–H bond of HRh(dppb)₂, reaction 5.



$$\Delta G^\circ_{\text{H}^-} = -1.37 \log K_{\text{eq}2} - 1.37 \text{p}K_{\text{a}(3)} + 76.0 \text{ kcal/mol} \quad (6)$$

The free energies associated with reactions 2 (–0.5 kcal/mol, –1.37 pK_{eq 2}), 3 (–41.6 kcal/mol, calculated using a pK_a value of 30.4 for [HPt(dmpp)₂]⁺),¹⁶ and 4 (76.0 kcal/mol, the free energy associated with the heterolytic cleavage of hydrogen in acetonitrile)^{17,18} can therefore be used in eq 6 to calculate the hydride donor ability, ΔG[°]_{H[–]}, of HRh(dppb)₂ (34 kcal/mol). The uncertainty of this value is estimated to be approximately ±1.4 kcal/mol on the basis of the uncertainty of the equilibrium constant (±0.8 kcal/mol) and the pK_a value of [HPt(dmpp)₂]⁺ (±0.6 kcal/mol).

Acidity of HRh(dppb)₂. The acidity of HRh(dppb)₂ can be calculated using eq 10. This equation is based on the sequence of reactions 5, 7, and 8. Reaction 5 is the hydride donor ability of HRh(dppb)₂, which was determined as described in the preceding paragraph. Reaction 7 is the reduction of [Rh(dppb)₂]⁺ to [Rh(dppb)₂][–] (E_{1/2} = –2.02 V vs ferrocene in acetonitrile), and reaction 8 is the oxidation of the hydride ion to H⁺ in acetonitrile (–79.6 kcal/mol when referenced to the ferrocene/ferrocenium couple).^{4a,18} The sum of these reactions is the deprotonation of HRh(dppb)₂, eq 9, and the free energy for this process is the sum of the free energies associated with these three reactions as shown in eq 10. The resulting free energy value of 47 kcal/mol corresponds to a pK_a value of 35 ± 1.3. The estimated uncertainty arises from the uncertainty in the free energy associated with reaction 5 (±1.4 kcal/mol) and the uncertainty in the reduction potential of reaction 7 (±0.4 kcal/mol).



$$\Delta G^\circ_{\text{H}^+} = \Delta G^\circ_{\text{H}^-} - 46.1E^\circ(\text{I}^-/\text{I}) - 79.6 \quad (10)$$

Discussion

Thermodynamic parameters have now been determined for a series of first, second, and third row

isoelectronic complexes of the formula [HM(diphosphine)₂]ⁿ⁺, where M = Co, Rh, n = 0, and M = Ni, Pt, n = 1.^{4,11,17} It has been necessary to introduce some slight variations in the diphosphine ligands used in the comparisons of this series. The dppe and dppb ligands appeared to be the most suitable for thermodynamic studies of the acidity and hydricity of the rhodium hydrides, because they are among the least electron donating commercially available diphosphine ligands. It was therefore anticipated that HRh(dppe)₂ and HRh(dppb)₂ would be less hydridic than most other HRh(diphosphine)₂ complexes. This feature is important because the determination of hydricity by the heterolytic cleavage of hydrogen required a base whose conjugate acid has a pK_a value of approximately 31. The base therefore had to be (1) a strong base, (2) noncoordinating to rhodium, and (3) not so bulky that the reaction was too slow for steric reasons. We were fortunate to find that Pt(dmpp)₂ fit these requirements, and HPt(dmpp)₂ reacted cleanly with HRh(dppb)₂ to give a readily measured equilibrium mixture as shown in reaction 2. Unfortunately, the reaction of HRh(dppe)₂ with the same platinum reagent resulted in ligand exchange and decomposition reactions, and an accurate equilibrium measurement was not possible for the dppe complex.

Acidities of M(III) Hydrides. The pK_a values of the rhodium(III) derivatives [HRh(dppe)₂(CH₃CN)]²⁺ (9.0 ± 0.3) and [HRh(dppb)₂(CH₃CN)]²⁺ (9.4 ± 0.3) are nearly the same, and both values are smaller than that of [HCo(dppe)₂(CH₃CN)]²⁺ (11.3).¹¹ The isoelectronic complexes HRh(dmg)₂(PPh₃) and HCo(dmg)₂(PBU₃) show a similar trend, with pK_a values of 9.5 and 10.5, respectively, in 50:50 water/methanol mixtures.^{2e} Comparisons of octahedral rhodium(III) and iridium(III) hydrides have been made in studies of oxidative addition reactions of protic acids to MX(CO)(PR₃)₂ complexes in methanol (where M = Rh or Ir and X = halide). The studies indicate that Rh complexes are also slightly more acidic (by 0 to 1 pK_a unit) than the analogous Ir complexes.^{2c} These data taken together would indicate that the differences in acidity between octahedral Co, Rh, and Ir complexes in the +3 oxidation state are small, with Rh hydrides being slightly more acidic than both the analogous Co and Ir derivatives. For the diphosphine complexes studied here, deprotonation is also accompanied by cleavage of the M–solvent bond. It may be that the small difference in pK_a values is a consequence of the loss of coordinated solvent molecules that accompanies the deprotonation of the octahedral complexes. In contrast, the isoelectronic octahedral complexes, H₂Fe(CO)₄, H₂Ru(CO)₄, and H₂Os(CO)₄, show a systematic decrease in acidity as one descends the periodic table with pK_a values of 11.4, 18.7, and 20.8, respectively, in acetonitrile.¹⁹ In this case no ligand loss accompanies deprotonation. It is clear that more data are needed to fully understand the factors governing the relative acidity within triads of metal octahedral complexes.

Acidities of M(I) Hydrides. The acidity of HRh(dppb)₂ (pK_a = 35) is greater than that observed for HCo(dppe)₂ (pK_a = 38).¹¹ The difference is due in part to the greater electron-withdrawing ability of the dppb

(18) Wayner, D. D. M.; Parker, V. D. *Acc. Chem. Res.* **1993**, *26*, 287–294.

(19) Moore, E. J.; Sullivan, J. M.; Norton, J. R. *J. Am. Chem. Soc.* **1986**, *108*, 2257. (b) Jordan, R. F.; Norton, J. R. *J. Am. Chem. Soc.* **1982**, *104*, 1255.

ligand relative to that of dppe. This is indicated by protonation experiments for these two ligands²⁰ and is supported by the electrochemical data for the Rh and Co complexes of these ligands. For example, the reversible Rh(I/–I) couple of [Rh(dppb)₂](BF₄) (–2.02 V) is slightly less negative than that of [Rh(dppe)₂](BF₄) (–2.12 V),⁹ and a similar trend is observed for the reversible Co(0/–I) couples in the cobalt analogues (–1.85 V for Co(dppb)₂²¹ vs –2.03 V for Co(dppe)₂.¹¹ Fortunately the difference introduced by the ligand variation can be estimated accurately. We have shown in previous work that a linear free energy correlation exists between the d⁹/d¹⁰ reduction potentials in the [M(diphosphine)₂]ⁿ⁺ complexes (where M = Co and Ni) and the pK_a values of their corresponding hydrides.^{4b} Using this correlation and an observed redox potential of –1.85 V for the Co(0/–I) couple of [Co(dppb)₂]⁺,²¹ we can predict that the pK_a of HCo(dppb)₂ is 35 ± 1. We conclude that for the same diphosphine ligand Rh(I) has approximately the same acidity as Co(I). Because [HPt(dppe)₂]⁺ (pK_a = 22.0) is much less acidic than [HNi(dppe)₂]⁺ (pK_a = 14.2),⁴ it would appear that the acidity decreases in the order second row ≥ first row > third row for isoelectronic [HM(diphosphine)₂]ⁿ⁺ complexes. These data are consistent with more qualitative observations that suggested the acidity order HRh(CO)₄ > HCo(CO)₄ > HIr(CO)₄.^{22,23} Unpublished data listed in a review by Norton for HM[P(OMe)₃]₄⁺ complexes also follow the acidity order Pd ≥ Ni > Pt.^{2a,23} For these triads of five-coordinate hydrides, all of the data are consistent with the same trend in acidity.

Hydricity of M(I) Hydrides. Previous work has also established that a linear free energy correlation exists between the d⁸/d⁹ reduction potentials in the [M(diphosphine)₂]ⁿ⁺ complexes (where M = Co and Ni) and the ΔG^o_{H–} values for their hydride derivatives. This correlation has been used to determine that ΔG^o_{H–} for HCo(dppb)₂ is 48 kcal. Our determination that ΔG^o_{H–} for HRh(dppb)₂ is 34 kcal/mol establishes that the rhodium complex is a better hydride donor than the cobalt analogue by 14 kcal/mol. The difference in hydride donor ability is significantly larger than the 10 kcal/mol difference between [HNi(dppe)₂]⁺ and [HPt(dppe)₂]⁺.^{4a} This larger difference implies that second row transition metal hydride complexes are also better hydride donors than third row metal hydrides. This suggests that hydricity follows the order second row > third row > first row for the [HM(diphosphine)₂]ⁿ⁺ complexes studied here. The data listed for the complexes shown in Table 3 demonstrate that the neutral HM(diphosphine)₂ complexes (where M = Co or Rh) are much more hydridic than their isoelectronic [HM'(diphosphine)₂]⁺ analogues (where M' = Ni and Pt).⁴ Although we have focused on the influence of the metal in this paper, it is worth noting that the effect of the ligands can outweigh that of the metals. For example, [HNi(dmpe)₂]⁺ is less acidic (pK_a = 24.3) and more

Table 3. ΔG^o (in kcal/mol) for Hydride Transfer in Acetonitrile^a

H ₂	76
[H ₂ -Co(dppe) ₂] ⁺	65
[H-Ni(dppe) ₂] ⁺	63
[H-Ni(dmpp) ₂] ⁺	61
[H-Co(dppe) ₂] ⁺	60
benzylnicotinamide	59
[H-Ni(depe) ₂] ⁺	56
[H-Pt(dppe) ₂] ⁺	52
H-Co(dppe) ₂	49
[H-Ni(dmpe) ₂] ⁺	48
[H-Pt(dmpp) ₂] ⁺	47
[HCO ₂] ⁻	43
[H-Pt(depe) ₂] ⁺	41
[H-Pt(dmpe) ₂] ⁺	39
H-Rh(dppb) ₂	34

^a Uncertainties for these values are estimated to be ±2 kcal/mol.

hydridic (ΔG^o_{H–} = 51 kcal/mol) than [HPt(dppe)₂]⁺ (22.0 and 52, respectively).

Conclusions. A comparison of the acidity and hydricity of HCo(dppe)₂ and HRh(dppb)₂ indicates that the rhodium hydride complex is both more hydridic and more acidic than the cobalt complex. On the basis of the other acidity and hydricity series discussed above, the result that second row transition metal complexes of the type HML₄ will be both more acidic and more hydridic than their first and third row analogues appears to be general. This is a clear indication that an increase in acidity is not necessarily accompanied by a decrease in hydricity. The decoupling of acidity and hydricity has also been discussed in a somewhat different sense by Labinger for Cp₂MH₂ and [Cp₂MH₃]⁺ complexes where M = Mo and W.²⁴ This interesting phenomenon of being simultaneously a good hydride and a good proton donor may be related to the higher catalytic activity sometimes observed for second row transition elements. A corollary to this observation is that second row HML₄ complexes will be stable over a smaller pK_a range.

A second observation from this study that deserves emphasis is the very hydridic character of five-coordinate Rh^(I) hydrides. HRh(dppb)₂, with a hydride donor ability of 34 kcal/mol, is the strongest hydride donor identified in our studies of the series of [HM(diphosphine)₂]ⁿ⁺ complexes. The rhodium complex significantly extends the ΔG^o values for these derivatives (Table 3), which now cover a range of >30 kcal/mol. HRh(dppb)₂ also displays significantly better hydride donor ability than other compounds that have been used for this function, including hydrogen,¹⁷ formate,²⁵ and benzylnicotinamide (a NADH analogue),²⁶ and quantitative comparisons are included in Table 3. Although further syntheses and studies of HRh(diphosphine)₂ derivatives were not pursued here, it is clear from previous work that hydride donor ability can be significantly enhanced by incorporating phosphine chelates with strong electron donor properties. Rhodium complexes with such ligands, e.g., [HRh(dmpe)₂]⁺ (where

(20) Sowa, J. R., Jr.; Angelici, R. J. *Inorg. Chem.* **1991**, *30*, 3534.

(21) The cyclic voltammogram of [Co(dppb)₂(CH₃CN)]₂[BF₄]₂ in CH₃CN/0.3 M Bu₄NBF₄ shows three reversible one-electron reductions at potentials of –0.66, –1.59, and –1.85 V vs Fc. However, because of low solubilities and the large quadrupole of cobalt, the compounds were not suitable for equilibrium studies by NMR techniques.

(22) Vidal, J. L.; Walker, W. E. *Inorg. Chem.* **1981**, *20*, 249.

(23) Tolman, C. A. *J. Am. Chem. Soc.* **1970**, *92*, 4217–4222.

(24) Labinger, J. A. In *Transition Metal Hydrides*; Dedieu, A., Ed.; VCH: New York, 1991; pp 361–379.

(25) DuBois, D. L.; Berning, D. E. *Appl. Organomet. Chem.* **2000**, *14*, 860–862.

(26) (a) Cheng, J-P.; Lu, Y.; Zhu, X.; Mu, L. *J. Org. Chem.* **1998**, *63*, 6108–6114. (b) Anne, A.; Moiroux, J. *Org. Chem.* **1990**, *55*, 4608–4614.

(27) van der Ent, A.; Onderdelinden, A. L. *Inorg. Synth.* **1973**, *XIV*, 92.

dmpe = 1,2-bis(dimethylphosphino)ethane), should be among the most powerful hydride donors available.

Summary

Comparison of the acidity and hydricity properties of $\text{HRh}(\text{dppb})_2$ with those of other five-coordinate metal hydrides studied previously leads to the conclusion that for isoelectronic complexes the hydricity varies in the order second row > third row > first row and acidity follows the sequence second row \geq first row > third row. As a result, we expect second row metal hydrides of this class to be both more hydridic and more acidic than their first and second row analogues. This should result in second row metal hydrides of this class being more reactive and less stable than their first and third row analogues. Finally, Rh(I) complexes were found to be powerful hydride donors.

Experimental Section

All reactions were performed under purified nitrogen with the use of standard Schlenk-line techniques. Manipulations of air-sensitive compounds were carried out in an UHP nitrogen-filled glovebox. All solvents were thoroughly dried and deoxygenated prior to use by refluxing under a nitrogen atmosphere over either CaH_2 or Na/benzophenone. Glassware was dried by heating under vacuum before use. Chemical analyses were performed by Desert Analytics Inc. Mass spectra were obtained on a Hewlett-Packard 5989A electrospray ionization LC mass spectrometer or on a Finnigan MATR LCQ ion trap mass spectrometer. IR spectra were recorded for KBr pellets on a Nicolet 510P spectrometer. ^1H , ^{31}P , $^{31}\text{P}\{^1\text{H}\}$, and $^{13}\text{C}\{^1\text{H}\}$ NMR spectra were recorded on a Varian Unity Inova 500 MHz spectrometer at 500.37, 202.55, and 125.83 MHz, respectively. ^1H and ^{13}C chemical shifts are reported relative to tetramethylsilane. ^{31}P chemical shifts are reported relative to external phosphoric acid. Cyclic voltammetry data were obtained under an atmosphere of nitrogen on 0.3 M Bu_4NBF_4 solutions in acetonitrile on a Cypress Systems computer-aided electrolysis system. The working electrode was a glassy carbon disk, and the counter electrode was a glassy carbon rod. An Ag/AgCl reference electrode was used to fix the potential. Ferrocene was used as an internal standard, and all potentials are referenced to the ferrocene/ferrocenium couple.

AgBF_4 , 1,2-bis(diphenylphosphino)benzene (dppb), $\text{HBF}_4 \cdot \text{Et}_2\text{O}$, 4-bromoaniline, LiAlH_4 , LiEt_3BD , and ferrocenium tetrafluoroborate were purchased from Aldrich Chemical Co. and used as received. 4-Bromoanilinium tetrafluoroborate was prepared by protonation of 4-bromoaniline using tetrafluoroboric acid. $[\text{Rh}(\text{dppe})_2][\text{BF}_4]$, $[\text{HRh}(\text{dppe})_2]$,⁸ and $\text{Pt}(\text{dmpp})_2$ ^{4a} were synthesized according to the literature procedures, and $[\text{Co}(\text{dppb})_2(\text{CH}_3\text{CN})][\text{BF}_4]_2$ and $[\text{HCo}(\text{dppb})_2][\text{BF}_4]$ were synthesized by procedures reported for the dppe derivatives.¹¹

$[\text{Rh}(\text{dppb})_2][\text{BF}_4]$. Stoichiometric amounts of $[\text{RhCl}(\text{C}_8\text{H}_{14})_2]_2$ ²⁷ (100 mg, 1.4×10^{-4} mol) and AgBF_4 (54 mg, 2.8×10^{-4} mol) were dissolved in acetone (20 mL) and allowed to stir for 1 h. The AgCl precipitate that formed was removed by filtration of the mixture through a short (1 cm) column of Celite directly into a solution of dppb (249 mg, 5.6×10^{-4} mol) in dichloromethane (20 mL). Material remaining on the column was washed through with further aliquots of acetone (2×5 mL). The orange homogeneous solution that formed was allowed to stir at room temperature for 1 h, followed by reduction of the solvent volume, in vacuo, to ca. 4 mL. Addition of diethyl ether (50 mL) afforded a yellow precipitate, which was filtered off and washed twice with diethyl ether (2×30 mL). Slow diffusion of diethyl ether into an acetonitrile solution (3 mL) of the product afforded a microcrystalline solid, $[\text{Rh}(\text{dppb})_2][\text{BF}_4]$, that was filtered off and dried overnight in vacuo

(255 mg, 84% yield). Anal. Found (calcd): C, 66.58 (66.56); H, 4.52 (4.47). Mass spectrum (electrospray): 995, $[\text{M} - \text{BF}_4]^+$, 100%. ^{31}P NMR (acetonitrile- d_3): 62.50 ppm (d, $^1J_{\text{P-H}} = 134$ Hz). ^1H NMR (acetonitrile- d_3): 7.04, 7.17, 7.41, and 7.48 ppm (multiplets, all aromatic ^1H 's).

$\text{HRh}(\text{dppb})_2$. A suspension of $[\text{Rh}(\text{dppb})_2][\text{BF}_4]$ (100 mg, 8.3×10^{-5} mol) and LiAlH_4 (100 mg, 2.6×10^{-3} mol) in toluene (25 mL) was stirred at room temperature for 48 h to produce a deep-red solution. The mixture was passed through a Celite column, which was washed with toluene (2×5 mL). The volume of the filtrate was reduced to ca. 5 mL in vacuo. Addition of diethyl ether (20 mL) and hexanes (30 mL) and cooling at -10 °C overnight produced a red precipitate (45 mg, 54% yield), which was collected by filtration and dried. Anal. Found (calcd): C, 68.23 (72.29); H, 5.04 (4.95). In repeated attempts, the analysis for carbon was low; however no impurities greater than 5% were observed by ^{31}P NMR or ^1H NMR spectroscopy or by cyclic voltammetry. Mass spectrum (MAL-DI): (996, $[\text{M}]^+$, 56%), (995, $[\text{M} - \text{H}]^+$, 100%). IR: $\nu(\text{RhH}) = 1868$ cm^{-1} . ^{31}P NMR (benzene- d_6): 59.30 ppm (dd, $^1J_{\text{P-Rh}} = 142$ Hz, $^2J_{\text{P-H}} = 18$ Hz). ^1H NMR (benzene- d_6): -9.39 ppm (d pentets, $^1J_{\text{Rh-H}} = 12$ Hz, $^2J_{\text{P-H}} = 18$ Hz); 6.78, 6.84, 6.95, 7.31, and 7.51 ppm (multiplets, aromatic ^1H 's).

$\text{DRh}(\text{dppb})_2$ was prepared by a similar procedure using excess LiEt_3BD . IR: $\nu(\text{RhD}) = 1343$ cm^{-1} . ^{31}P NMR (benzene- d_6): 59.3 ppm (d, $J_{\text{Rh-P}} = 142$ Hz). The ^1H NMR was identical to that reported above for $\text{HRh}(\text{dppb})_2$, except the hydride resonance was absent.

$[\text{HRh}(\text{diphosphine})_2(\text{CH}_3\text{CN})][\text{BF}_4]_2$. To a solution of $[\text{Rh}(\text{dppb})_2][\text{BF}_4]$ (100 mg, 8.3×10^{-5} mol) in acetonitrile (20 mL) was added $\text{HBF}_4 \cdot \text{Et}_2\text{O}$ (13.9 μL , 8.6×10^{-5} mol, in diethyl ether) by syringe. The yellow hue of the starting material, $[\text{Rh}(\text{dppb})_2][\text{BF}_4]$, disappeared within minutes to give a colorless solution, which was stirred for an hour at room temperature. The solvent volume was reduced in vacuo to ca. 3 mL, followed by addition of diethyl ether (50 mL). The white precipitate, $[\text{HRh}(\text{dppb})_2(\text{CH}_3\text{CN})][\text{BF}_4]_2$, that formed was filtered off and washed with diethyl ether (2×20 mL). Recrystallization from an acetonitrile/diethyl ether mixture afforded crystals suitable for X-ray crystallographic studies (92 mg, 82% yield). Anal. Found (calcd) for $\text{C}_{62}\text{H}_{52}\text{N}_4\text{P}_4\text{B}_2\text{F}_8\text{Rh}$: C, 60.52 (61.47); H, 4.47 (4.37); N, 1.23 (1.16). Mass spectrum (electrospray): 995, $[\text{M} - (\text{BF}_4)_2 - \text{H} - \text{CH}_3\text{CN}]^+$, 100%. IR: $\nu(\text{RhH}) = 1993$ cm^{-1} (tentative). ^{31}P NMR (acetonitrile- d_3): 56.85 ppm (dd, $^1J_{\text{P-Rh}} = 93$ Hz, $^2J_{\text{P-H}} = 7.5$ Hz). ^1H NMR (acetonitrile- d_3): -14.56 ppm (d pentets, $^1J_{\text{Rh-H}} = 10$ Hz, $^2J_{\text{P-H}} = 7.5$ Hz, Rh-H), 2.00 ppm (s, coordinated CH_3CN), 7.28, 7.39, 7.48, 7.56, 7.68, and 7.75 (multiplets, all aromatic ^1H 's).

An identical procedure was used for the synthesis of $[\text{HRh}(\text{dppe})_2(\text{CH}_3\text{CN})][\text{BF}_4]_2$. Anal. Found (calcd): for $\text{C}_{54}\text{H}_{55}\text{N}_4\text{P}_4\text{B}_2\text{F}_8\text{Rh} + 1 \text{CH}_3\text{CN}$: C, 58.02 (58.15); H, 4.74 (4.79); N, 2.29 (2.42). ^{31}P NMR (acetonitrile- d_3): 56.03 ppm (dd, $^1J_{\text{P-Rh}} = 92$ Hz, $^2J_{\text{P-H}} = 7$ Hz). ^1H NMR (acetonitrile- d_3): -15.9 ppm (d pentets, $^1J_{\text{Rh-H}} = 11$ Hz, $^2J_{\text{P-H}} = 11$ Hz, Rh-H).

pK_a Determination of $[\text{HRh}(\text{dppb})_2(\text{CH}_3\text{CN})][\text{BF}_4]_2$ in Acetonitrile. Four independent experiments were performed to determine the pK_a of $[\text{HRh}(\text{dppb})_2(\text{CH}_3\text{CN})][\text{BF}_4]_2$. Two solutions were prepared in CD_3CN containing 20:20:1 molar ratios of 4-bromoaniline:4-bromoanilinium tetrafluoroborate: $[\text{HRh}(\text{dppb})_2(\text{CH}_3\text{CN})][\text{BF}_4]_2$. Similarly two solutions were prepared containing 20:20:1 molar ratios of 4-bromoaniline: 4-bromoanilinium tetrafluoroborate: $[\text{Rh}(\text{dppb})_2(\text{BF}_4)]$. The reactions were followed by ^{31}P NMR spectroscopy, and constant ratios of $[\text{HRh}(\text{dppb})_2(\text{CH}_3\text{CN})][\text{BF}_4]_2$ to $[\text{Rh}(\text{dppb})_2(\text{BF}_4)]$ were observed after 1 h. Integrations for equilibrium measurements were recorded after 24 h.

Reaction of $[\text{Rh}(\text{dppb})_2(\text{BF}_4)]$ with H_2 and $\text{Pt}(\text{dmpp})_2$. $[\text{Rh}(\text{dppb})_2(\text{BF}_4)]$ and $\text{Pt}(\text{dmpp})_2$ (approximately 1×10^{-2} mmol of each) were added to an NMR tube. This mixture of solids was dissolved in benzonitrile (approximately 1 mL), and an insert filled with D_2O was used for a lock signal. H_2 gas (620

mmHg, atmospheric pressure at 5400 ft of elevation) was bubbled through the solution for approximately 0.5 h, and ³¹P NMR spectra were recorded periodically over the course of 12 h. After approximately 3 h an equilibrium was reached, as indicated by a constant ratio of products. Integration of each of the resonances of the four different species present provided the ratios required for calculating equilibrium constants. An equilibrium constant of 0.42 ± 0.2 was measured for the reverse of reaction 2 in a series of four experiments.

Heterolytic Cleavage of H₂ with Pt(dmpp)₂(PF₆)₂ in Benzonitrile. To compare equilibrium constants for heterolytic H₂ cleavage in benzonitrile and acetonitrile, the following experiment involving reagents soluble in both solvents was carried out. Pt(dmpp)₂(PF₆)₂ (22–28 mg, 0.027–0.034 mmol), HNEt₃BF₄ (52–78 mg, 0.28–0.41 mmol), and NEt₃ (33–42 mg, 0.33–0.42 mmol) were accurately weighed into three NMR tubes and benzonitrile containing 10% CD₃CN (0.7 mL) was added to each. The tubes were capped with septa, and H₂ was slowly bubbled through a needle into each solution for 10 min to produce a saturated solution at 1 atm (620 mmHg). The solutions were resaturated with H₂ daily. The reactions were monitored by ³¹P NMR spectroscopy until equilibrium was reached (5 days in this case). The concentrations of Pt(dmpp)₂²⁺ and HPt(dmpp)₂⁺ at equilibrium were determined by integrating the ³¹P resonances of these complexes. The concentrations of NEt₃ and HNEt₃⁺ used in each case were high enough that they were not changed significantly by the reaction. The equilibrium constant for the reaction was then calculated using the measured concentrations of the Pt-containing species and the known [HNEt₃⁺]/[NEt₃] ratio. The average value for the equilibrium constant from the three samples was 3.2 ± 0.5 , which gives a hydride donor ability (ΔG_{H^-}) for HPt(dmpp)₂⁺ of 51.4 kcal/mol in benzonitrile. This compares to an equilibrium constant of 1.7 ± 0.3 in acetonitrile for this complex and a ΔG_{H^-} of 51.0 kcal/mol.^{4a}

X-ray Diffraction Study of [HRh(dppb)₂(CH₃CN)](BF₄)₂·2CH₃CN. Crystals were examined under a light hydrocarbon oil and mounted with silicone vacuum grease. The mounted assembly was transferred to the goniometer of a Siemens SMART CCD diffractometer equipped with a locally modified LT-2A low-temperature apparatus operating at 130 K.

Cell parameters were determined using reflections harvested from three orthogonal sets of 20 0.3° ω scans. Final cell parameters were refined using 19 681 reflections with $I > 10\sigma(I)$ chosen from 62 340 in the entire data set. An arbitrary hemisphere of data was collected to 0.68 Å using 0.3° ω scans measured for 30 s in two correlated 30 s exposures. Data were truncated to 0.80 Å during refinement due to poor agreement at higher resolution; 100% of the unique data was measured. All data were corrected for Lorentz and polarization effects, as well as for absorption.

Structure solution via direct methods in centrosymmetric space group *P* $\bar{1}$ revealed the non-hydrogen component of this structure. There are two independent molecules in the asymmetric unit. Subsequent least-squares refinement followed with calculation of difference Fourier maps exposed disorder in the position of the BF₄ anions. Each of these was successfully modeled. All non-hydrogen atoms were refined with parameters for anisotropic thermal motion. Hydride, H1, was located by difference map and freely refined in subsequent cycles of least squares. Remaining hydrogen atoms were placed at calculated geometries and allowed to ride on the position of the parent atom. Hydrogen thermal parameters were set to 1.2 times the equivalent isotropic thermal parameter of the parent atom. Largest features in the final difference electron density map, 1.56 e⁻/Å³, were located near the disordered anions.

Acknowledgment. This research was supported by the National Science Foundation, Grant 9981835. D.L.D. and C.J.C. would also like to acknowledge the support of the United States Department of Energy, Office of Basic Energy Sciences, Division of Chemical Sciences.

Supporting Information Available: Complete details of the X-ray diffraction studies on [HRh(dppb)₂(CH₃CN)](BF₄)₂·2CH₃CN. This material is available free of charge via the Internet at <http://pubs.acs.org>.

OM020421K